Research Article

# Facile Synthesis of Glutathione-Copper Nanoparticles for 3-Monochloropropanediol Colorimetric Detection

Yora Faramitha, Firda Dimawarnita and Irma Kresnawati
Indonesian Oil Palm Research Institute–Bogor Unit, Jl. Taman Kencana No 1 Bogor, West Java, Indonesia

Muhammad Hanif Ainun Azhar
Center for Sustainability and Waste Management, Universitas Indonesia, Depok, West Java, Indonesia

Havid Aqoma
Kelip-kelip!, Center of Excellence for Light Enabling Technologies, School of Energy and Chemical Engineering, Xiamen University Malaysia, Selangor, Malaysia
Energy Conversion & Storage (EnergONS) Group, School of Energy and Chemical Engineering, Xiamen University Malaysia, Selangor, Malaysia

Alfian Ferdiansyah
Department of Metallurgical and Materials Engineering, Faculty of Engineering, Universitas Indonesia, Depok, West Java, Indonesia

Adam Febriyanto Nugraha*
Department of Metallurgical and Materials Engineering, Faculty of Engineering, Universitas Indonesia, Depok, West Java, Indonesia
Advanced Materials Research Center, Faculty of Engineering, Universitas Indonesia, Depok, West Java, Indonesia

* Corresponding author. E-mail: adam.febriyanto04@ui.ac.id DOI: 10.14416/j.asep.2024.11.005
Received: 5 August 2024; Revised: 30 September 2024; Accepted: 8 October 2024; Published online: 14 November 2024


**Abstract**
3-Monochloropropanediol (MCPD) is a carcinogen compound commonly found in refined cooking oil, including palm oil. The high risk of human intoxication increases the importance of 3-MCPD detection. This study proposes the optimum chemical reduction synthesis condition of colloidal copper nanoparticles functioned by L-glutathione (GSH-Cu NPs) as an alternative accessible 3-MCPD detector used in the colorimetric method. The volume of copper source, capping agent, and reducing agent were optimized to find the optimum synthesis formula. 3.6 mL of 3 mM $CuCl_2$, 25 µL of 20 mM L-glutathione (GSH), and 150 µL hydrazine hydrate were found to be the best combination to form GSH-Cu NPs; the combination made the sharpest UV-Vis absorption peak. Fourier Transform Infrared (FTIR) spectrometry measurement confirmed the reaction and encapsulation of Cu NPs with GSH. Transmission Electron Microscopy (TEM) and Particle Size Analyzer (PSA) observations revealed the quasi-spherical morphology of the nanoparticles, with an average size of 51.3 nm. The sample withstood 1:1 dilution with deionized water and maintained its dispersion and distribution after 10 days. The fabricated GSH-Cu NPs were able to detect 3-MCPD until 50 ppm. This study aimed to provide insight into the synthesis of copper nanoparticles as non-precious metals for the application of 3-MCPD colorimetric detection.

**Keywords**: Colorimetric detection, Copper nanoparticles, L-glutathione, 3-MCPD, Refined palm oil

## 1 Introduction

Oil as a whole constitute can be defined as the hydrophobic liquid that is extracted from various sources. Naturally derived oil is called natural oils, which can be derived from various biomass, such as seeds, roots, woods, leaves, flowers, to fruit [1]. Various natural oil products are used on a daily basis, such as canola oil, rice bran oil, corn oil, rapeseed oil, olive oil, soybean oil, and cottonseed oil [2]–[4]. Oil palm, from the *Elaeis* genus, is one of the world's primary commodities due to its diverse application potential, being used in food products, oleochemical, biodiesel, and hydrogen production [5]–[7]. Capitalizing on its suitable environment to grow oil palm, Indonesia led the world in oil palm production with more than 45 million metric tons of crude palm oil (CPO) plus nearly 10 million metric tons of palm kernel in 2022 [8]. The industry also notably contributed to the nation's export income, with over 27 billion USD received from exporting more than half of nationwide annual CPO production [8], [9].

CPO undergoes several processes to be converted into refined, bleached, and deodorized palm oil (RBDPO), namely the deodorizing process [10]–[12]. The process utilizes chlorinated water and high temperature (200–270 °C), which can form a reaction with acylglycerols in the oil to form 3-monochloropropanediol (3-MCPD) [12]–[15]. Research proved that hydrolyzed free form of 3-MCPD acts as a probable carcinogen, and it may affect the kidney, neurological and cardiovascular systems, as well as male fertility [11], [13], [15]. Due to the potentially dangerous effect of 3-MCPD, the European Food Safety Agency (EFSA) prescribed a low maximum 3-MCPD total daily intake (TDI) of 0.2 to 0.7 µg/kg of body weight [16]. While the European Commission had stated the maximum content of 2.5 mg 3-MCPD/kg, palm oil still contains over-the-limit 3-MCPD inside [11], [15], [17]. Almoselhy *et al*., found 5.6 mg 3-MCPD/kg of palm oil in their 2021 study, the highest out of 8 edible oils [17]. Due to the severe potential risk of 3-MCPD contamination to the human system, 3-MCPD detection for the palm oil industry becomes important to limit the excessive-3-MCPD-containing palm oil products released to the market.

Various methods can detect 3-MCPD in organic substances. Tang *et al*., studied 3-MCPD content in soy sauce using high-performance liquid chromatography-tandem mass spectroscopy (HPLC-MS/MS) [18]. They quantified the 3-MCPD content of 11 different commercial soy sauces and found that several samples contained significantly higher 3-MCPD content than allowed by the EU. The previously mentioned study by Almoselhy *et al*., determined the 3-MCPD content in edible oils via gas chromatography-tandem triple quadrupole mass spectroscopy (GC-MS/MS) [17]. The electrochemical method was used by Martin *et al*., and Cheng *et al*., in their respective investigations, using Cys-Ag NPs modified gold and nanoporous gold/glass carbon as their electrode, respectively [19], [20]. However, the aforementioned methods are more expensive, complicated, and usually located *ex situ*, making immediate detection improbable. Therefore, colorimetric analysis serves as an alternative for a simpler, cost-efficient, and accessible detection method.

Colorimetric analysis works by capitalizing on the unique localized surface plasmon resonance (LSPR) of conductive nanoparticles, which can be observed by the naked eye or using a UV-Vis spectrophotometer [21], [22]. Martin *et al*., studied the use of Cys-Ag nanoparticles for 3-MCPD detection [23]. The synthesized nanoparticles can detect 3-MCPD by bare observation and colorimetric detection. At 100 °C and 9.3 pH level, Cys-Ag nanoparticles could detect 3-MCPD in only 5 minutes. Mahardika *et al*., conducted another 3-MCPD colorimetric detection study using silver nanoparticles, in which they found that both new and used cooking oil contained higher 3-MCPD than the allowed limit [24]. Gold nanoparticles were also widely used in biological and chemical colorimetric sensors [25]. The use of precious metals for colorimetric detection is deemed cost-inefficient. Thus, copper nanoparticle is proposed as an alternative material for 3-MCPD colorimetry due to its comparable optical properties yet cheaper [26], [27].

In this study, the chemical reduction method was used to make colloidal copper nanoparticles. The presence of a capping agent is necessary to prevent copper oxidation during the reduction process [28]. L-glutathione (GSH) was used as the capping agent in this study to get GSH-Cu nanoparticles (NPs). Hydrazine hydrate was used as a reducing agent. Salt precursor, capping agent, and reducing agent volume were varied to find the optimum synthesis condition. The synthesis environment was also studied, comparing the results under an ambient environment to results under an inert environment. Application studies – dilution effect and aging – were done to further analyze the feasibility of using GSH-Cu NPs in 3-MCPD colorimetric detection. The optimum sample was then used for colorimetric detection of 3-MCPD. This study hopes to give meaningful insight

into the synthesis of an alternative less-expensive material applied for 3-MCPD nanoparticle colorimetric detection.

## 2 Materials and Methods

### 2.1 *Reagents and chemicals*

Copper (II) chloride ($CuCl_2$) was obtained from Merck. L-glutathione reduced ($C_{10}H_{17}N_3O_6S$, GSH), hydrazine hydrate (80% solution in water, $N_2H_4•H_2O$), and 3-chloro-1,2-propanediol ($C_3H_7ClO_2$, 3-MCPD) were purchased from Sigma-Aldrich. Deionized (DI) water was purified by Milli-DI from Merck Millipore. All chemicals and reagents were used without further purification and treatment unless stated otherwise.

### 2.2 *GSH-Cu NPs synthesis optimization*

To optimize the synthesis process of GSH-Cu NPs, the volume of $CuCl_2$ precursor, capping agent, and reducing agent were varied. $CuCl_2$ precursor and capping agent concentration were kept constant at 3 mM and 20 mM, respectively. Each variable was studied independently, leading to a total of 11 samples synthesized. The studied variables are listed in Table 1.

**Table 1**: Sample synthesis variables.

| Optimization Stages | Component Volume | | |
|---|---|---|---|
| | $CuCl_2$ (3 mM) | GSH (20 mM) | Hydrazine Hydrate |
| Optimization of $CuCl_2$ concentration | 3.0 mL<br>3.6 mL<br>4.0 mL<br>4.5 mL | 20 µL | 200 µL |
| Optimization of GSH concentration | 3.6 mL | 20 µL<br>25 µL<br>30 µL | 200 µL |
| Optimization of Hydrazine hydrate concentration | 3.6 mL | 25 µL | 100 µL<br>150 µL<br>200 µL<br>250 µL |

To synthesize the GSH-Cu NPs, a set amount of 3 mM $CuCl_2$ was diluted with 8 mL DI water. The solution was then stirred at 400 rpm and heated with a magnetic stirrer (Cimarec Stirring Hot Plate, Thermo Scientific). After reaching 70 °C, GSH with the intended volume was added. Further heating was done until 80 °C when hydrazine hydrate was added according to the set experiment being done. The solution temperature and stirring speed were maintained at 80 °C and 400 rpm while the solution was left to react for 30 min until homogeneous nanoparticles colloid was formed. Additional scale-up feasibility studies were done using nitrogen as an environmental variable, as well as dilution and aging to measure the nanoparticles' stability and resiliency.

### 2.3 *GSH-Cu NPs characterization*

To confirm the formation of GSH-Cu NPs, UV-Vis spectrophotometry analysis (MULTISKAN GO Microplate Spectrophotometer, Thermo Scientific) was employed to detect the absorption peak of the samples. The detection was done from 500 to 800 nm under room temperature.

Further sample characterization was done by Fourier Transform Infrared (FTIR) spectrometry (Nicolet iS5 FTIR Spectrometer) to identify functional groups comprising the samples. The FTIR measurement was done at 4000 to 400 $cm^{-1}$, with DTGS KBr and KBr as the detector and beam splitter, respectively.

The nanoparticles' morphology and size were observed by Transmission Electron Microscopy (TEM, FEI Tecnai G2 20S-Twin) and the particle size was further verified by Particle Size Analyzer (PSA, Zetasizer NANO ZS, Malvern Panalytical).

### 2.4 *3-MCPD colorimetric detection*

Colorimetric detection was done with the help of a UV-Vis spectrophotometer. 8 mL of 10, 50, or 100 ppm 3-MCPD was added drop-by-drop to 2 mL of GSH-Cu NPS colloid in a vial. After setting the mixture for 1 h, the absorption of the mixture was measured by the UV-Vis spectrophotometer.

## 3 Results and Discussions

### 3.1 *GSH-Cu NPs synthesis optimization*

Figure 1(a) shows the UV-Vis measurement result of samples with varied copper precursor volumes. The peak locations and intensity are detailed in Table 2. A peak is visible at 592 nm when 3.6 mL of 3 mM $CuCl_2$ was used in the mixture (red) while using lower and higher precursor volume led to flat curves without any peak. Several studies have reported various locations of Cu(0) peak, which are generally positioned at around 550 to 650 nm [29]–[33]. Therefore, the peak located at 592 nm indicated the formation of GSH-Cu NPs. Quintero-Quiroz *et al.*, in their 2019 study, suggested the presence of an optimum point of silver precursor concentration to produce maximum yield

[34]. A smaller amount of precursor limited the amount of metal ions to be reduced, meaning less formation of nanoparticles [35]. Meanwhile, extra precursor induced the aggregation of nanoparticles, leading to settlement and less reading sensitivity from the spectrophotometer [36]. This result suggests that this experiment's optimum copper precursor volume is 3.6 mL.

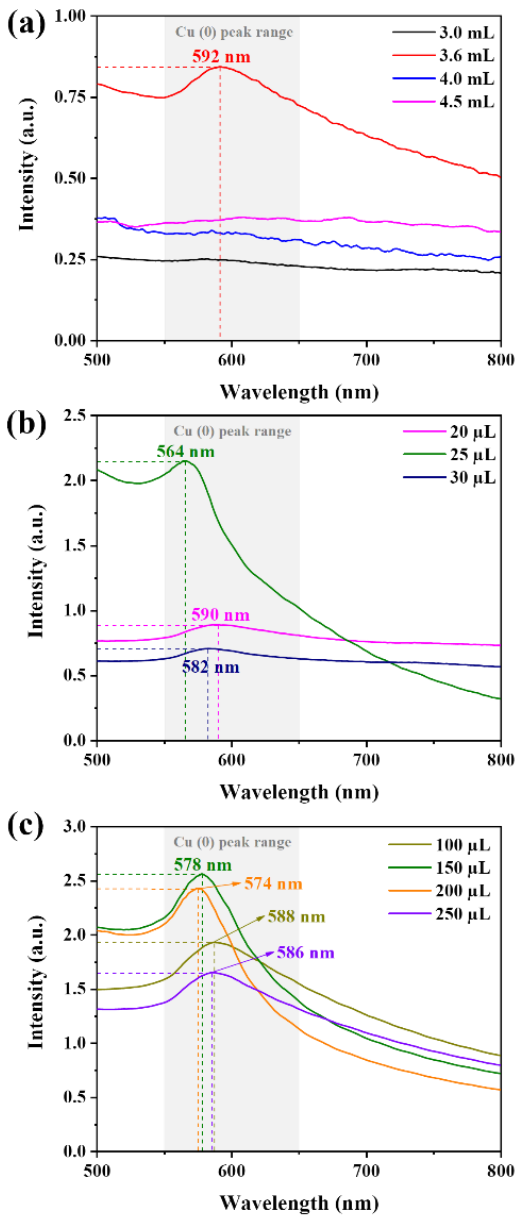


**Figure 1**: UV-Vis spectra of GSH-Cu NPs with varied volumes of (a) $CuCl_2$, (b) glutathione, and (c) hydrazine hydrate.

**Table 2**: Peak position and intensity of each optimization sample.

| Optimization Stages | Component Volume | Peak Position | Intensity |
|---|---|---|---|
| Optimization of $CuCl_2$ concentration | 3.0 mL | - | - |
| | 3.6 mL | 592 nm | 0.84 |
| | 4.0 mL | - | - |
| | 4.5 mL | - | - |
| Optimization of GSH concentration | 20 µL | 590 nm | 0.89 |
| | 25 µL | 564 nm | 2.15 |
| | 30 µL | 582 nm | 0.71 |
| Optimization of Hydrazine hydrate concentration | 100 µL | 588 nm | 1.93 |
| | 150 µL | 578 nm | 2.56 |
| | 200 µL | 574 nm | 2.42 |
| | 250 µL | 586 nm | 1.65 |

Figure 1(b) displays the UV-Vis measurement results for different GSH volumes used during the chemical reduction process. A noticeably sharper peak appeared for the 25 µL sample (green), while wider peaks appeared for the 20 µL and 30 µL samples, represented by purple and dark-blue lines, respectively. Peak-shifting was also observed, where the peak blue-shifted from the 20 µL sample to the 25 µL sample, then red-shifted again slightly in the 30 µL sample. The initial increase of capping agent volume leads to smaller and more uniform nanoparticles, leading to a clearer peak and blue-shifting [37]–[39]. Further addition of a capping agent might form a larger shell layer of the nanoparticles, increasing the size of the nanoparticles [40]. From these results, 25 µL of GSH is deemed to be the optimum amount of capping agent for this study.

Using the optimum $CuCl_2$ and GSH volume, the reducing agent variations were studied. The UV-Vis measurement results are illustrated in Figure 1(c). The addition of a reducing agent sharpened the peak and shifted the peak location. When the more reducing agent was added, the peak widened and red-shifted. Increasing the amount of reducing agent can induce a faster reaction, leading to smaller nanoparticles and shifting of UV-Vis peak location [41]. However, the excess reducing agent might turn to enlarge the nanoparticle's size, broadening the UV-Vis absorption peak [42]. Thus, the optimum hydrazine hydrate addition was 150 µL (olive-colored).

### 3.2 *GSH-Cu NPs characterization*

The previous results hinted at the optimum composition for making GSH-Cu NPs. The samples for future observations were then fabricated using 3.6 mL of 3 mM $CuCl_2$, 25 µL of 20 mM GSH, and 150 µL 80 % hydrazine hydrate. First, UV-Vis was tried to

confirm the presence of GSH-Cu NPs (Figure 2(a)). The intense peak exhibited at 578 nm in the figure proved the presence of Cu(0) in the colloid [29]–[33]. FTIR measurement was conducted to further affirm the GSH was incorporated in the colloidal nanoparticles. Figure 2(b) shows the FTIR spectra of GSH and GSH-Cu NPs. Notable peaks for GSH are located at 3337.95 $cm^{-1}$, 2514.88 $cm^{-1}$, 1592. 28 $cm^{-1}$ and 1532.71 $cm^{-1}$ for $NH_3^+$ stretching, –SH stretching, and C=O stretching, respectively [43], [44]. The absence of –SH peak in the GSH-Cu NPs indicates the linkage between the sulfur atom from the capping agent to the nanoparticles [45]. Three peaks at around 2800 to 3000 $cm^{-1}$ and 1058.99 $cm^{-1}$ of GSH-Cu NPs were assigned to be C–H stretching vibration and metal–O stretching [46]. The rest of the peaks were observed at the same range albeit with less intensity, indicating there were no extra reactions between the protective capping agent and the protected Cu clusters, which reduced the intensity of the intrinsic GSH peaks [47]. These peaks confirmed the encapsulation of Cu nanoparticles with the GSH capping agent.

TEM observation in Figure 3(a) displays the morphology and particle size of the synthesized GSH-Cu NPs. The images show quasi-spherical nanoparticles with around 50 nm in size. The particle size analysis result shown in Figure 3(b) also confirmed the average size of the nanoparticles was 51.3 nm.

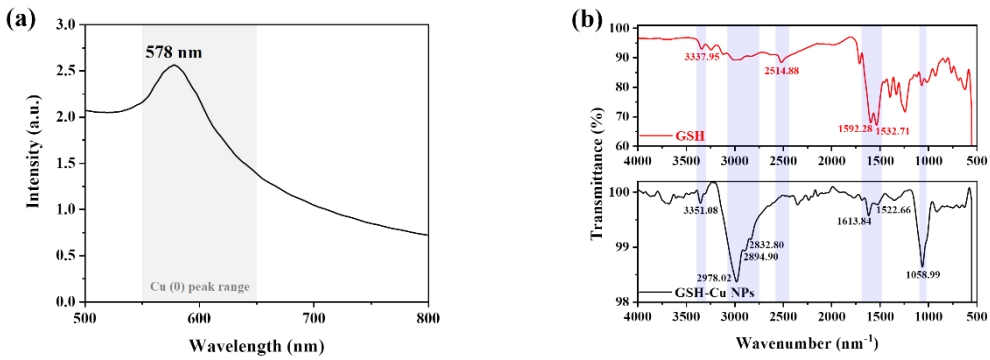


**Figure 2**: (a) UV-Vis measurement of GSH-Cu NPs and (b) FTIR analysis of reduced L-glutathione and GSH-Cu NPs.

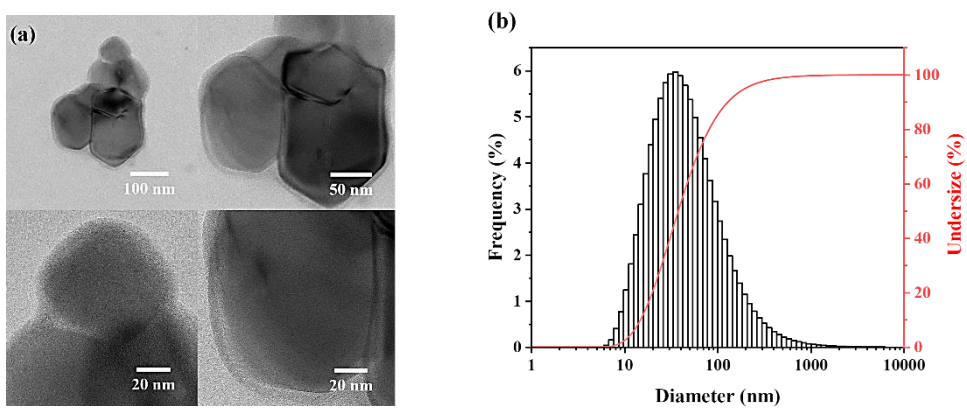


**Figure 3**: (a) TEM images and (b) PSA analysis of GSH-Cu NPs

### 3.3 *GSH-Cu NPs scale-up feasibility*

The feasibility studies were conducted on the optimum GSH-Cu NPs. First, the study explored the necessity of an inert environment to synthesize the colloidal nanoparticles. Under an inert environment, the peak shown in Figure 4(a) is more profound than the peak under an ambient environment. However, the ambient environment still produced a distinct peak. The lack of

additional cost under an ambient environment will add to the bigger-scale application feasibility.

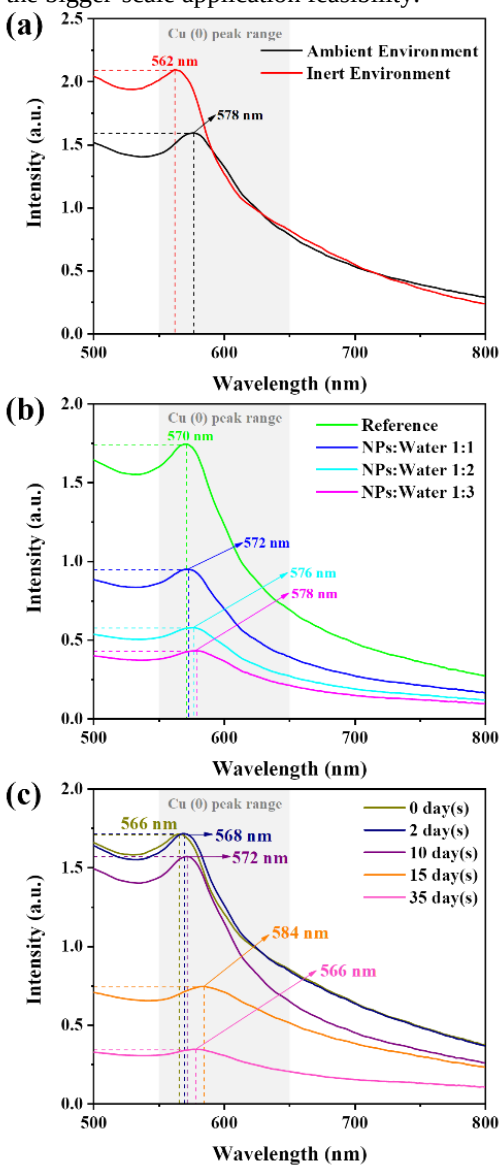


**Figure 4**: UV-Vis measurement of (a) GSH-Cu NPs synthesized under varied environments, (b) Diluted nanoparticle colloid, and (c) GHS-Cu NPs stability.

A dilution study was done to see the limit at which the colloid still contains nanoparticles. By adding more DI water, the peak widened, as seen in Figure 4(b). The peak intensity is still detectable until the addition of 1-part DI water to the colloid. This indicates the resiliency of the nanoparticles to maintain their dispersion and distribution after dilution, which is necessary for colorimetric detection. The peaks were still located in the same region, showing no reaction with the addition of water.

The effect of aging was observed to see the stability of the nanoparticles after being left for several days. Figure 4(c) shows the compiled UV-Vis measurement results of several GSH-Cu NPs samples after aging. The sample still maintained its peak intensity after 10 days when the peak flattened significantly after 15 days and 35 days. Peak flattening and red-shifting can be attributed to nanoparticle agglomeration, variety in size and amount, as well as the degradation of the nanoparticle [41], [48], [49]. The synthesized nanoparticles showed relatively good stability after 10 days.

### 3.4 *3-MCPD colorimetric detection*

The optimum GSH-Cu NPs colloid nanoparticles were used in the colorimetric detection of 3-MCPD. The 3-MCPD detection is displayed in Figure 5. The UV-Vis peak was flattened after 3-MCPD addition, with the 100 ppm peak being the flattest out of the three samples (inset of Figure 5). Peak widening and red-shifting were also observed, indicating the disturbance in the GSH-Cu NPs by the 3-MCPD [46], [50], [51]. The similar level of intensity between 10 and 50 ppm samples might indicate the detection limitation of the nanoparticles, hence a respectable detection limit.

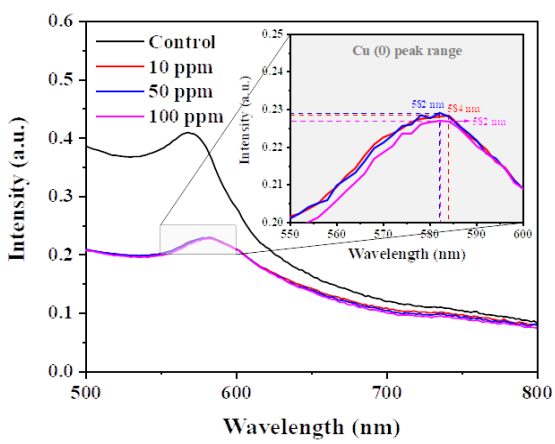


**Figure 5**: UV-Vis measurement results of GSH-Cu NPs with varied 3-MCPD dose addition.

## 4 Conclusions

The selected synthesis method was successful in synthesizing GSH-Cu NPs. Three volume parameters affected the formation of GSH-Cu NPs: copper salt,

capping agent, and reducing agent. Copper salt as the copper ion source will be reduced to zero-valence copper by the reducing agent. Additional capping agents ensured the protection of the nanoparticles from oxidation. Optimum values for the parameters were found and proven via several characterization modes.

UV-Vis absorption measurement indicated the formation of Cu NPs using 3.6 mL of $CuCl_2$, 20 µL of GSH, and 200 µL Hydrazine hydrate. Additionally, with further optimization stages, a more robust formula of 3.6 mL $CuCl_2$, 25 µL GSH, and 150 µL Hydrazine yielded a more prominent peak, therefore indicative of the most optimum formula.

FTIR analysis confirmed the bond between GSH capping agent to Cu NPs, signified by the absence of the GSH-intrinsic –SH peak and the presence of C–H and metal–O peaks in the GSH-Cu NPs FTIR peak. From the TEM observation, the optimized sample has a quasi-spherical shape with an average 51.3 nm particle size as measured by PSA analysis. Scaling-up the nanoparticle usage was simply measured, resulting in the sample resisting 1:1 water dilution and 10 days of aging. The proposed nanoparticles can be used to detect 3-MCPD up to 50 ppm. With a respectable detection limit and good scale-up possibility, the proposed nanoparticles can be further developed for end-goal usage for in-situ 3-MCPD detection.

## Acknowledgments

This research was supported by The Indonesian Palm Oil Plantation Fund Management Agency (BPDPKS) contract number PRJ-24/DPKS/2021 and Hibah Publikasi Terindeks Internasional (PUTI) Q2 2023-2024 No. NKB-794/UN2.RST/HKP.05.00/2023.

## Author Contributions

Y.F.: conceptualization, investigation, formal analysis, resources, writing – original draft; F.D.: conceptualization, formal analysis, resources; M.H.A.A.: formal analysis, writing – original draft, visualization; H.A.: validation, writing – review & editing; I.K.: formal analysis, investigation; A.F: conceptualization, validation, writing – review & editing; A.F.N.: validation, writing – review & editing, supervision, project administration, funding acquisition.

## Conflicts of Interest

The authors declare no conflict of interest.

## References

[1] S. Baptista-Silva, S. Borges, O. L. Ramos, M. Pintado, and B. Sarmento, "The progress of essential oils as potential therapeutic agents: a review," *Journal of Essential Oil Research*, vol. 32, no. 4, pp. 279–295, Jul. 2020, doi: 10.1080/10412905.2020.1746698.

[2] V. Sharma and P. P. Kundu, "Addition polymers from natural oils—A review," *Progress in Polymer Science*, vol. 31, no. 11, pp. 983–1008, Nov. 2006, doi: 10.1016/j.progpolymsci.2006.09.003.

[3] T. M. T. Nguyen and H. V. H. Nguyen, "Enzymatic assisted treatments of lycopene extraction from tomato (*Lycopersicon Esculentum*) peels using rice bran oil," *Applied Science and Engineering Progress*, vol. 17, no. 1, Aug. 2023, Art. no. 6916, doi: 10.14416/j.asep.2023.08.003.

[4] L. Simasatitkul, S. Amornraksa, K. Katam, and S. Assabumrungrat, "Bio-jet fuel from vegetable oils: production process and perspective on modeling and simulation," *Applied Science and Engineering Progress*, vol. 17, no. 3, Jun. 2024, Art. no. 7415, doi: 10.14416/j.asep.2024.06.013.

[5] O. Farobie and E. Hartulistiyoso, "Palm oil biodiesel as a renewable energy resource in indonesia: current status and challenges," *BioEnergy Research*, vol. 15, no. 1, pp. 93–111, Mar. 2022, doi: 10.1007/s12155-021-10344-7.

[6] H. Limaho, Sugiarto, R. Pramono, and R. Christiawan, "The need for global green marketing for the palm oil industry in Indonesia," *Sustainability*, vol. 14, no. 14, Jul. 2022, Art. no. 8621, doi: 10.3390/su14148621.

[7] Z. Fona, I. Irvan, R. Tambun, F. Fatimah, A. Setiawan, and A. Adriana, "Review on advance catalyst for biomass gasification," *Applied Science and Engineering Progress*, vol. 17, no. 2, Jan. 2024, Art. no. 7295, doi: 10.14416/j.asep. 2024.01.001.

[8] Direktorat Statistik Tanaman Pangan, Hortikultura, dan Perkebunan, "Statistik Kelapa Sawit Indonesia 2022." bps.go.id. https://www.bps.go.id/id/publication/2023/11/30/160f211bfc4f91e1b77974e1/statistik-kelapa-sawit-indonesia-2022.html (accessed Jul., 2024)

[9] E. Cisneros, K. Kis-Katos, and N. Nuryartono, "Palm oil and the politics of deforestation in

Indonesia," *Journal of Environmental Economics and Management*, vol. 108, Jul. 2021, Art. no. 102453, doi: 10.1016/j.jeem.2021.102453.

[10] Badan Pengelola Dana Perkebunan Kelapa Sawit, "MENGENAL 3-MCPD dan GE," MENGENAL 3-MCPD dan GE. bpdp.or.id. https://www.bpdp.or.id/mengenal-3-mcpd-dan-ge (accessed Jul., 2024)

[11] K. S. Hew, Y. P. Khor, T. B. Tan, M. M. Yusoff, O. M. Lai, A. J. Asis, F. A. Alharthi, I. A. Nehdi, and C. P. Tan, "Mitigation of 3-monochloropropane-1,2-diol esters and glycidyl esters in refined palm oil: A new and optimized approach," *LWT*, vol. 139, Mar. 2021, Art. no. 110612, doi: 10.1016/j.lwt.2020.110612.

[12] J. Elisabeth, "Mitigation of 3-MCPDE and GE in palm oil in Indonesia," *E-Journal Menara Perkebunan*, vol. 91, no. 2, Oct. 2023, doi: 10.22302/iribb.jur.mp.v91i2.549.

[13] A. Eisenreich, B. H. Monien, M. E. Götz, T. Buhrke, A. Oberemm, K. Schultrich, K. Abraham, A. Braeuning, and B. Schäfer, "3-MCPD as contaminant in processed foods: State of knowledge and remaining challenges," *Food Chemistry*, vol. 403, Mar. 2023, Art. no. 134332, doi: 10.1016/j.foodchem.2022.134332.

[14] L. Peng, C. Yang, C. Wang, Q. Xie, Y. Gao, S. Liu, G. Fang, and Y. Zhou, "Effects of deodorization on the content of polycyclic aromatic hydrocarbons (PAHs), 3-monochloropropane-1,2-diol esters (3-MCPDE) and glycidyl esters (GE) in rapeseed oil using ethanol steam distillation at low temperature," *Food Chemistry*, vol. 413, Jul. 2023, Art. no. 135616, doi: 10.1016/j.foodchem.2023.135616.

[15] S. S. Syed Putra, W. J. Basirun, A. A. M. Elgharbawy, M. Hayyan, W. Al Abdulmonem, A. S. M. Aljohani, and A. Hayyan, "3-Monochloropropane-1,2-diol (3-MCPD): A review on properties, occurrence, mechanism of formation, toxicity, analytical approach and mitigation strategy," *Food Measure*, vol. 17, no. 4, pp. 3592–3615, Aug. 2023, doi: 10.1007/s11694-023-01883-y.

[16] EFSA Panel on Contaminants in the Food Chain (CONTAM), H. K. Knutsen, J. Alexander, L. Barregård, M. Bignami, B. Brüschweiler, S. Ceccatelli, B. Cottrill, M. Dinovi, L. Edler, B. Grasl-Kraupp, L. (Ron) Hoogenboom, C. S. Nebbia, I. P. Oswald, A. Petersen, M. Rose, A. Roudot, T. Schwerdtle, C. Vleminckx, G. Vollmer, H. Wallace, A. Lampen, I. Morris, A. Piersma, D. Schrenk, M. Binaglia, S. Levorato, and C. Hogstrand, "Update of the risk assessment on 3-monochloropropane diol and its fatty acid esters," *EFSA Journal*, vol. 16, no. 1, Jan. 2018, doi: 10.2903/j.efsa.2018.5083.

[17] R. Almoselhy, M. Eid, W. Abd El-Baset, and A. Aboelhassan, "Determination of 3-MCPD in some edible oils using GC-MS/MS," *Egyptian Journal of Chemistry*, vol. 64, no. 3, pp. 1639–1652, Mar. 2021, doi: 10.21608/ejchem.2021.64084.3373.

[18] Y. Tang, G. Yang, X. Liu, L. Qin, W. Zhai, E. K. Fodjo, X. Shen, Y. Wang, X. Lou, and C. Kong, "Rapid sample enrichment, novel derivatization, and high sensitivity for determination of 3-Chloropropane-1,2-diol in soy sauce via high-performance liquid chromatography–tandem mass spectrometry," *Journal of Agricultural and Food Chemistry*, vol. 71, no. 41, pp. 15388–15397, Oct. 2023, doi: 10.1021/acs.jafc.3c05230.

[19] A. A. Martin, E. K. Fodjo, Z. V. Eric-Simon, Z. Gu, G. Yang, T. Albert, C. Kong, and H.-F. Wang, "Cys-AgNPs modified gold electrode as an ultrasensitive electrochemical sensor for the detection of 3-chloropropane-1,2-diol," *Arabian Journal of Chemistry*, vol. 14, no. 9, Sep. 2021, Art. no. 103319, doi: 10.1016/j.arabjc.2021.103319.

[20] W. Cheng, Q. Zhang, D. Wu, Y. Yang, Y. Zhang, and X. Tang, "A facile electrochemical method for rapid determination of 3-chloropropane-1,2-diol in soy sauce based on nanoporous gold capped with molecularly imprinted polymer," *Food Control*, vol. 134, Apr. 2022, Art. no. 108750, doi: 10.1016/j.foodcont.2021.108750.

[21] Y. Wu, J. Feng, G. Hu, E. Zhang, and H.-H. Yu, "Colorimetric sensors for chemical and biological sensing applications," *Sensors*, vol. 23, no. 5, Mar. 2023, Art. no. 2749, doi: 10.3390/s23052749.

[22] E. Mauriz, "Clinical applications of visual plasmonic colorimetric sensing," *Sensors*, vol. 20, no. 21, Oct. 2020, Art. no. 6214, doi: 10.3390/s20216214.

[23] A. A. Martin, E. K. Fodjo, G. B. I. Marc, T. Albert, and C. Kong, "Simple and rapid detection of free 3-monochloropropane-1,2-diol based on cysteine modified silver nanoparticles," *Food Chemistry*, vol. 338, Feb. 2021, Art. no. 127787, doi: 10.1016/j.foodchem.2020.127787.

[24] R. G. Mahardika, F. A. Putri, Syarmila, F. Rizal, Guskarnali, and Henri, "Silver nanoparticle-

based biosensor as a rapid test for the detection 3-monochloropropane-1,2-diol (3-MCPD) in cooking oil," *IOP Conference Series: Earth and Environmental Science*, vol. 1267, no. 1, Dec. 2023, Art. no. 012101, doi: 10.1088/1755-1315/1267/1/012101.

[25] C.-C. Chang, C.-P. Chen, T.-H. Wu, C.-H. Yang, C.-W. Lin, and C.-Y. Chen, "Gold nanoparticle-based colorimetric strategies for chemical and biological sensing applications," *Nanomaterials*, vol. 9, no. 6, Jun. 2019, Art. no. 861, doi: 10.3390/nano9060861.

[26] N. Wang, Z. Han, H. Fan, and S. Ai, "Copper nanoparticles modified graphitic carbon nitride nanosheets as a peroxidase mimetic for glucose detection," *RSC Advances*, vol. 5, no. 111, pp. 91302–91307, 2015, doi: 10.1039/C5RA18957H.

[27] B. Liu, J. Zhuang, and G. Wei, "Recent advances in the design of colorimetric sensors for environmental monitoring," *Environmental Science: Nano*, vol. 7, no. 8, pp. 2195–2213, 2020, doi: 10.1039/D0EN00449A.

[28] R. A. Soomro, A. Nafady, Sirajuddin, N. Memon, T. H. Sherazi, and N. H. Kalwar, "l-cysteine protected copper nanoparticles as colorimetric sensor for mercuric ions," *Talanta*, vol. 130, pp. 415–422, Dec. 2014, doi: 10.1016/j.talanta.2014.07.023.

[29] D. Deng, Y. Cheng, Y. Jin, T. Qi, and F. Xiao, "Antioxidative effect of lactic acid-stabilized copper nanoparticles prepared in aqueous solution," *Journal of Materials Chemistry*, vol. 22, no. 45, pp. 23989–23995, 2012, doi: 10.1039/c2jm35041f.

[30] A. Pérez-de León, J. Plasencia, A. Vázquez-Durán, and A. Méndez-Albores, "Comparison of the in vitro antifungal and anti-fumonigenic activities of copper and silver nanoparticles against *Fusarium verticillioides*," *Journal of Cluster Science*, vol. 31, no. 1, pp. 213–220, Jan. 2020, doi: 10.1007/s10876-019-01638-0.

[31] K. R. Shubhashree, R. Reddy, A. K. Gangula, G. S. Nagananda, P. K. Badiya, S. S. Ramamurthy, P. Aramwit, and N. Reddy, "Green synthesis of copper nanoparticles using aqueous extracts from *Hyptis suaveolens* (L.)," *Materials Chemistry and Physics*, vol. 280, Mar. 2022, Art. no. 125795, doi: 10.1016/j.matchemphys.2022.125795.

[32] S. S. Biresaw and P. Taneja, "Copper nanoparticles green synthesis and characterization as anticancer potential in breast cancer cells (MCF7) derived from Prunus *nepalensis* phytochemicals," *Materials Today: Proceedings*, vol. 49, pp. 3501–3509, 2022, doi: 10.1016/j.matpr.2021.07.149.

[33] M. Tiwari, P. Jain, R. Chandrashekhar Hariharapura, K. Narayanan, U. Bhat K., N. Udupa, and J. V. Rao, "Biosynthesis of copper nanoparticles using copper-resistant *Bacillus cereus*, a soil isolate," *Process Biochemistry*, vol. 51, no. 10, pp. 1348–1356, Oct. 2016, doi: 10.1016/j.procbio.2016.08.008.

[34] C. Quintero-Quiroz, N. Acevedo, J. Zapata-Giraldo, L. E. Botero, J. Quintero, D. Zárate-Triviño, J. Saldarriaga, and V. Z. Pérez, "Optimization of silver nanoparticle synthesis by chemical reduction and evaluation of its antimicrobial and toxic activity," *Biomaterials Research*, vol. 23, no. 1, Dec. 2019, Art. no. 27, doi: 10.1186/s40824-019-0173-y.

[35] J. Belloni, J.-L. Marignier, and M. Mostafavi, "Mechanisms of metal nanoparticles nucleation and growth studied by radiolysis," *Radiation Physics and Chemistry*, vol. 169, Apr. 2020, Art. no. 107952, doi: 10.1016/j.radphyschem.2018.08.001.

[36] T. M. D. Dang, T. T. T. Le, E. Fribourg-Blanc, and M. C. Dang, "Synthesis and optical properties of copper nanoparticles prepared by a chemical reduction method," *Advances in Natural Sciences: Nanoscience and Nanotechnology*, vol. 2, no. 1, Mar. 2011, Art. no. 015009, doi: 10.1088/2043-6262/2/1/015009.

[37] M. Maliki, I. H. Ifijen, E. U. Ikhuoria, E. M. Jonathan, G. E. Onaiwu, U. D. Archibong, and A. Ighodaro, "Copper nanoparticles and their oxides: optical, anticancer and antibacterial properties," *International Nano Letters*, vol. 12, no. 4, pp. 379–398, Dec. 2022, doi: 10.1007/s40089-022-00380-2.

[38] Z. S. Pillai and P. V. Kamat, "What factors control the size and shape of silver nanoparticles in the citrate ion reduction method?," *The Journal of Physical Chemistry B*, vol. 108, no. 3, pp. 945–951, Jan. 2004, doi: 10.1021/jp037018r.

[39] E. A. Mohamed, "Green synthesis of copper & copper oxide nanoparticles using the extract of seedless dates," *Heliyon*, vol. 6, no. 1, Jan. 2020, Art. no. e03123, doi: 10.1016/j.heliyon.2019.e03123.

[40] Z. Niu and Y. Li, "Removal and utilization of capping agents in nanocatalysis," *Chemistry of Materials*, vol. 26, no. 1, pp. 72–83, Jan. 2014, doi: 10.1021/cm4022479.

[41] T. U. Rajalakshmi, T. Reena, A. Doss, T. A. Kumar, T. A. Alahmadi, S. A. Alharbi, R. Mariselvam, and P. K. Mideen, "Evidence on temperature and concentration of reducing agents to control the nanoparticles growth and their microbial inhibitory efficacy," *Materials Research Express*, vol. 10, no. 3, Mar. 2023, Art. no. 035002, doi: 10.1088/2053-1591/acbf08.

[42] G. Villaverde-Cantizano, M. Laurenti, J. Rubio-Retama, and R. Contreras-Cáceres, "Reducing agents in colloidal nanoparticle synthesis – an introduction," in *Reducing Agents in Colloidal Nanoparticle Synthesis*, S. Mourdikoudis, Ed. London, UK: The Royal Society of Chemistry, pp. 1–27, 2021, doi: 10.1039/9781839163623-00001.

[43] S. N. Nyamu, L. Ombaka, E. Masika, and M. Ng'ang'a, "One-pot microwave-assisted synthesis of size-dependent L -glutathione-capped spherical silver nanoparticles suitable for materials with antibacterial properties," *Journal of Interdisciplinary Nanomedicine*, vol. 4, no. 3, pp. 86–94, Sep. 2019, doi: 10.1002/jin2.62.

[44] S. Bertoni, B. Albertini, C. Facchini, C. Prata, and N. Passerini, "Glutathione-loaded solid lipid microparticles as innovative delivery system for oral antioxidant therapy," *Pharmaceutics*, vol. 11, no. 8, Jul. 2019, Art. no. 364, doi: 10.3390/pharmaceutics11080364.

[45] M. Farrag and R. A. Mohamed, "Ecotoxicity of ∼1 nm silver and palladium nanoclusters protected by l -glutathione on the microbial growth under light and dark conditions," *Journal of Photochemistry and Photobiology A: Chemistry*, vol. 330, pp. 117–125, Nov. 2016, doi: 10.1016/j.jphotochem.2016.07.027.

[46] S. Sadeghi and M. Hosseinpour-Zaryabi, "Sodium gluconate capped silver nanoparticles as a highly sensitive and selective colorimetric probe for the naked eye sensing of creatinine in human serum and urine," *Microchemical Journal*, vol. 154, May 2020, Art. no. 104601, doi: 10.1016/j.microc.2020.104601.

[47] M. Farrag, "Preparation, characterization and photocatalytic activity of size selected platinum nanoclusters," *Journal of Photochemistry and Photobiology A: Chemistry*, vol. 318, pp. 42–50, Mar. 2016, doi: 10.1016/j.jphotochem.2015.11.023.

[48] H. I. Badi'ah, F. Seedeh, G. Supriyanto, and A. H. Zaidan, "Synthesis of silver nanoparticles and the development in analysis method," *IOP Conference Series: Earth and Environmental Science*, vol. 217, Jan. 2019, Art. no. 012005, doi: 10.1088/1755-1315/217/1/012005.

[49] W. Jin, G. Liang, Y. Zhong, Y. Yuan, Z. Jian, Z. Wu, and W. Zhang, "The influence of ctab-capped seeds and their aging time on the morphologies of silver nanoparticles," *Nanoscale Research Letters*, vol. 14, no. 1, Dec. 2019, Art. no. 81, doi: 10.1186/s11671-019-2898-x.

[50] G. Ma, J. Cao, G. Hu, L. Zhu, H. Chen, X. Zhang, J. Liu, J. Ji, X. Liu, and C. Lu, "Porous chitosan/partially reduced graphene oxide/ diatomite composite as an efficient adsorbent for quantitative colorimetric detection of pesticides in a complex matrix," *The Analyst*, vol. 146, no. 14, pp. 4576–4584, 2021, doi: 10.1039/ D1AN00621E.

[51] H. Li, H. Bai, Q. Lv, W. Wang, Z. Wang, H. Wei, and Q. Zhang, "A new colorimetric sensor for visible detection of Cu(II) based on photoreductive ability of quantum dots," *Analytica Chimica Acta*, vol. 1021, pp. 140–146, Aug. 2018, doi: 10.1016/j.aca.2018.03.011.